Supporting Information

Potentiometric *In Situ* Monitoring of Anions in the Synthesis of Copper and Silver Nanoparticles Using the Polyol Process

Jesse L. Carey III,[a] David R. Whitcomb,[b] Suyue Chen,[a] R. Lee Penn,[a] and Philippe Bühlmann*,[a]

[a]Department of Chemistry, University of Minnesota, 207 Pleasant Street SE, Minneapolis, Minnesota 55455, United States and [b]Carestream Health, 1 Imation Way, Oakdale, Minnesota 55128, United States

Assembly of the Reference Electrode

A custom-made, double-junction reference electrode was prepared from a glass tube that had a 5 mm outer diameter, at the bottom, and widened, to 10 mm, top. A 5 mm diameter porous glass frit was attached to the bottom of this tube using Teflon heat-shrink tubing. The glass tube was then filled with outer filling solution (propylene glycol saturated with KNO_3). A second 5 mm tube, with no taper and a porous glass frit attached to its lower end, was inserted into the outer filling solution and filled with the inner filling solution (propylene glycol saturated with KCl). A AgCl-coated Ag wire was inserted into the latter as an internal reference element.

Figure S1. Photographs of the reference electrode.

Design of the Ion-Selective Electrode

The dimensions of the ISE were as follows: shaft diameter, 10 mm; cap diameter, 13 mm; cap opening, 8 mm.

Figure S2. Photographs of the ISE as seen from the side and from the bottom on the left and right, respectively.

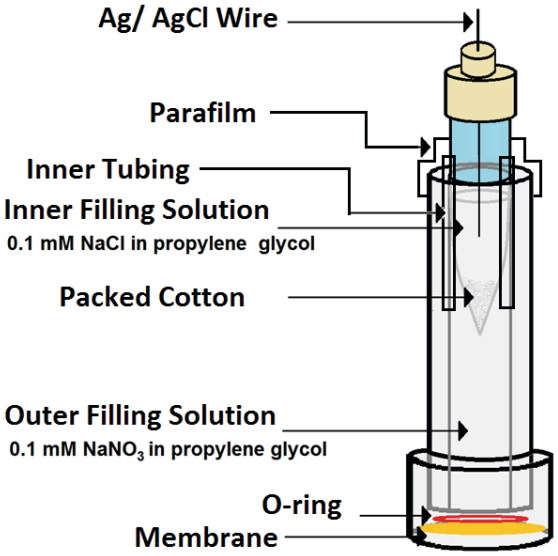

Figure S3. ISE schematic.

We found that gas bubbles that were trapped on the surface of the electrode can cause large changes in the measured potential, which can be explained by a very large increase in the resistance of the electrochemical cell when bubbles are present. To illustrate this effect, we bubbled nitrogen gas through an aqueous solution with varying concentrations of the electrolyte. When one or several bubbles large enough to block most of the surface of the sensing membrane became trapped under the electrode, the potential increased significantly. When this bubble subsequently was removed, the potential quickly returned to the pre-bubble value (Figure S4). Note that the data shown in Figure S7 were taken with the screw cap of the electrode completely immersed into the sample solution. We note that the potential increase is even larger (>1 V) when the electrode cap is only partially submerged into the sample solution (*i.e.*, when the area where the electrode screw cap and the main piece of the electrode body meet is not exposed to the sample). This suggests that there is stray impedance associated with minute volumes of sample solution trapped in between the screw cap and the main body of the ISE. This stray impedance does not interfere with the proper functioning of the electrode, but it affects the extent of the potential increase when bubbles completely block the sensing membrane of the ISE.
Two steps were taken to stop this effect from biasing the results of *in situ* measurements in the nanoparticle synthesis reactions in which bubbles form. First, the lip on the bottom of the electrode cap was reduced in size and cut to taper slightly outward (Figure S5). Second, the electrode was held in the reaction vessel at approximately 45° from horizontal. This setup was tested by bubbling nitrogen gas through the cell from underneath the electrode. No buildup of bubbles on the electrode surface was observed, and the measured emf was unaffected. Using this setup, we no longer observed potential changes due to the buildup of bubbles during nanoparticle synthesis reactions.

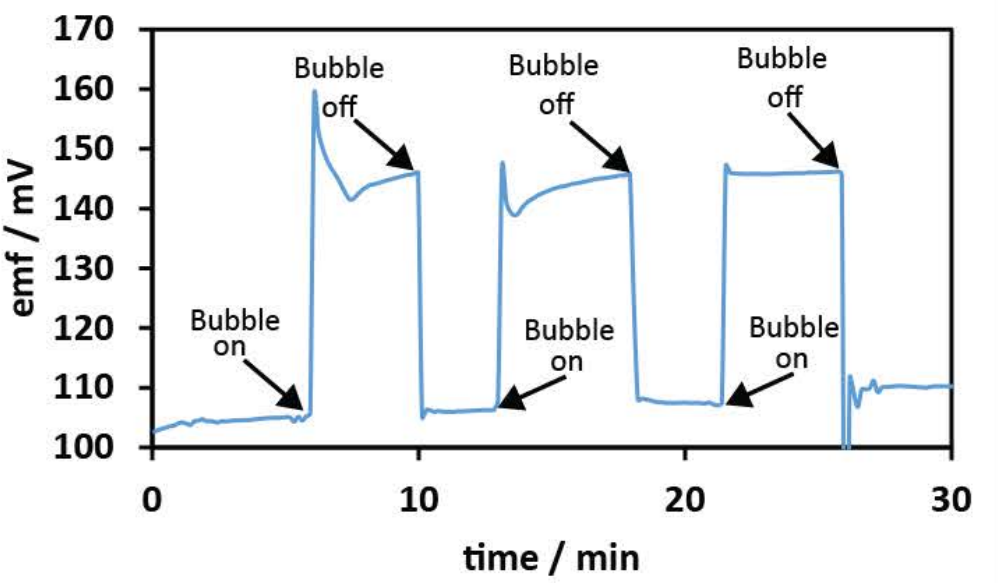

Figure S4. Effect of bubbles on the AHO electrode potential in 5 mM $NaNO_{3\,(aq)}$.

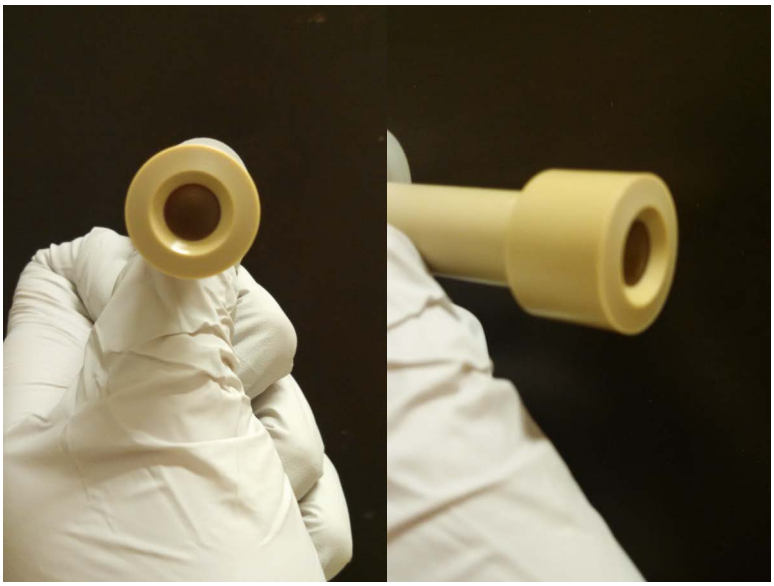

Figure S5. Electrode screw cap modified to eliminate effect of gas bubbles on the measured potential.

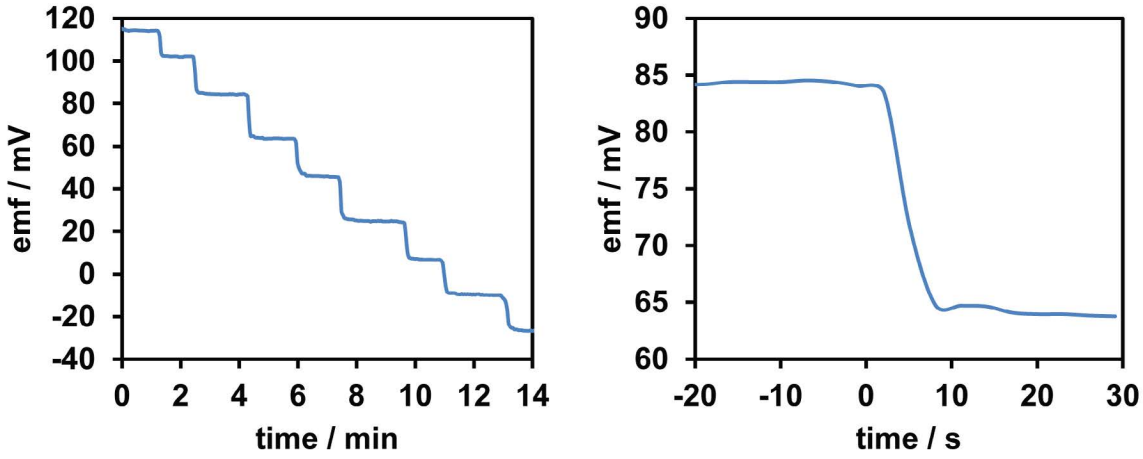

Figure S6. AHO electrode response to changing nitrate condition in propylene glycol at 150 °C, Left: response after several additions of NO_3^- changing concentration from 0.046 mM to 21.273 mM Right: response when changing [NO_3^-] from 0.221mM to 0.471 mM at t = 0, response time of less than 10 s

DSC Measurements

All ion exchangers were characterized using differential scanning calorimetry using a TA Instruments Q1000 (New Castle, DE, USA). The temperature was cycled from –20 ºC to 200 ºC, several times, with a scan rate of 10 ºC/min. The FAB and the AMI-7001S membranes were received dry, and no treatment prior to the DSC measurements was performed. The AHO membrane was received immersed in a solution and was rinsed with deionized water, blotted dry, and allowed to dry for 24 h before the DSC measurements were taken. See Figures S6 through S8 for plots of the temperature scans. The AHO membrane was subject to additional heating test in which it was heated to 150 ºC for multiple cycles with a heating rate of 1 ºC. The temperature was held at 150 ºC during each cycle for 5 m before continuing. The reproducibility between cycles is high excluding the first heating cycle. The differences between in the heat flow is likely due to the difference in the heating rate.

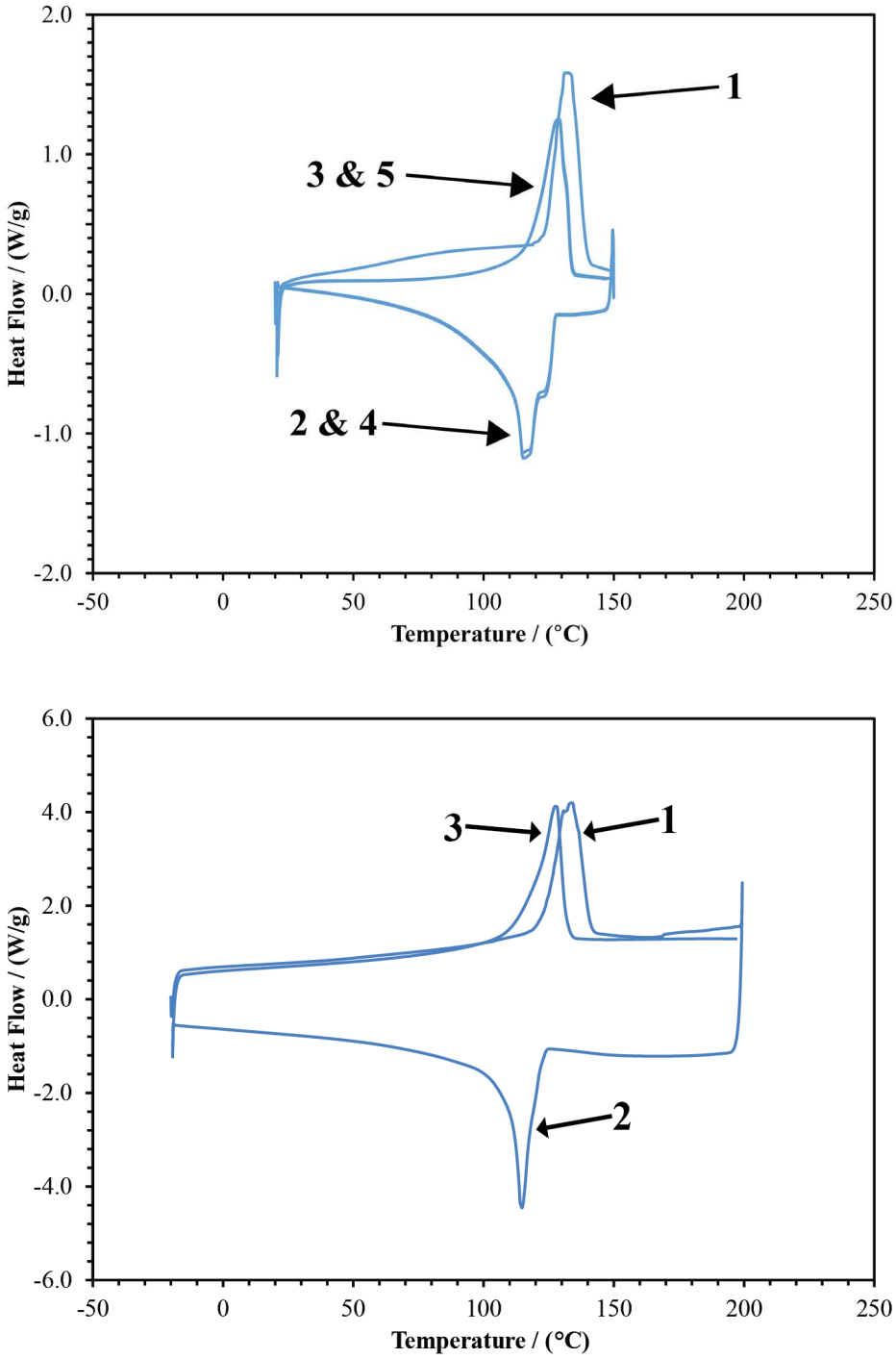

Figure S7. Top: DSCs of AHO membranes with a scan rate of 1 ºC/min heated and held there for 5 min for each cycle. DSCs of AHO membranes with a scan rate of 10 ºC/min to 200 ºC. Odd numbers refer to the first and third segments of the DSC scan (from a low to high temperature), and the even numbers refer to the second and fourth segments (from a high to low temperature).

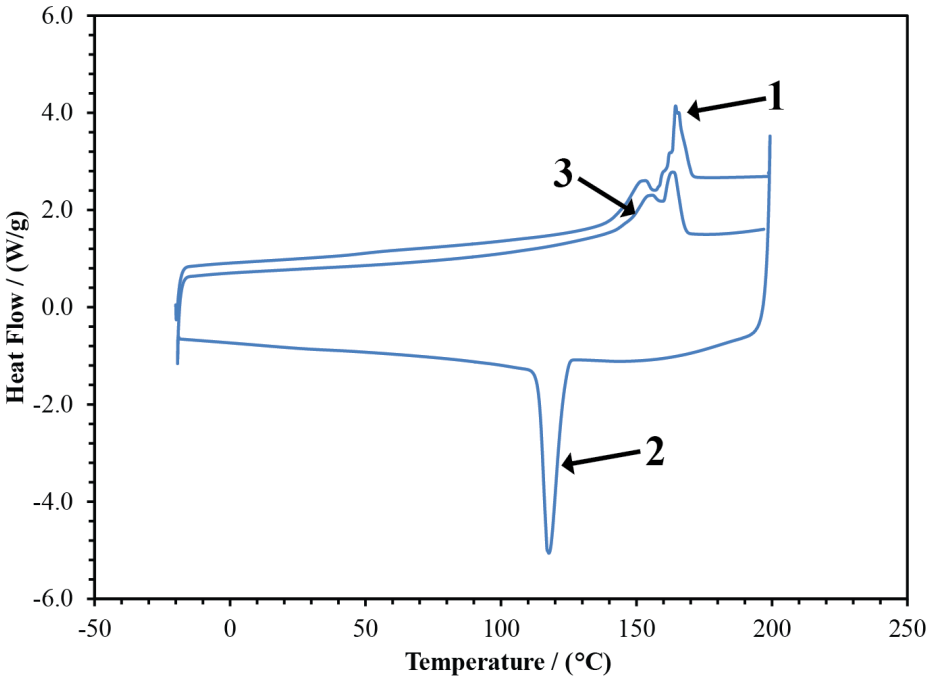

Figure S8. The DSC of the AMI membrane with a scan rate of 10 ºC/min. Odd numbers refer to the first and third segments of the DSC scan (from –20 to 200 ºC), and the number 2 refers to the second segment (from 200 to –20 ºC).

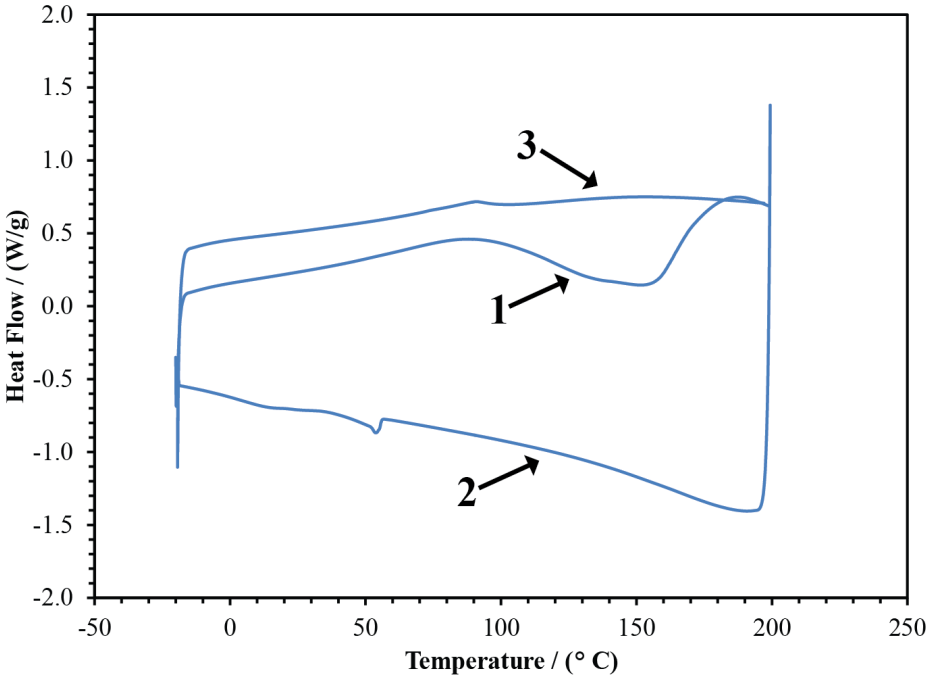

Figure S9. DSC of a FAB membrane with a scan rate of 10 ºC/min. Odd numbers refer to the first and third segments of the DSC scan (from –20 to 200 ºC), and the number 2 refers to the second segment (from 200 to –20 ºC).

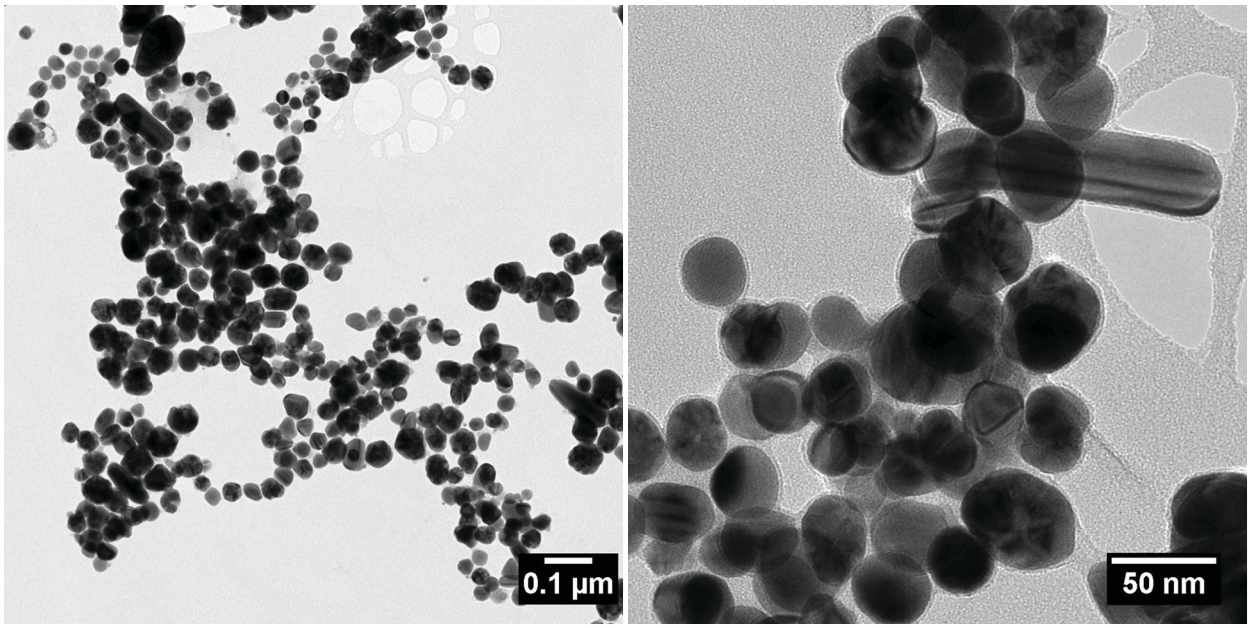

Figure S10. TEM images of silver nanoparticles

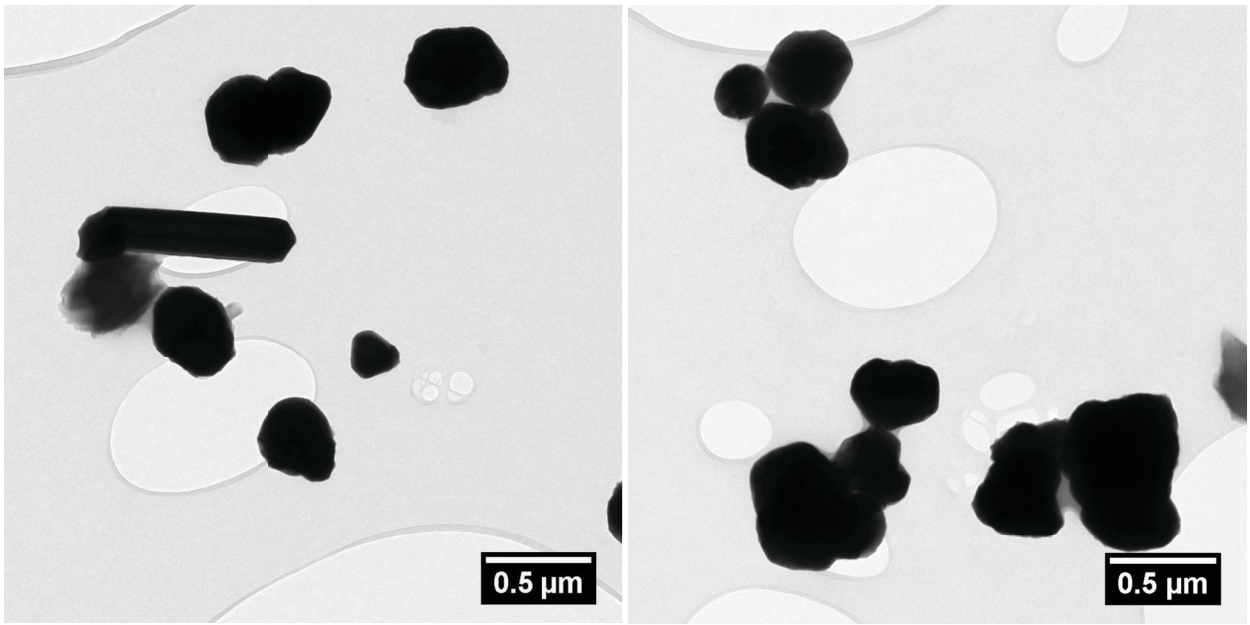

Figure S11. TEM images of copper nanoparticles

Table S1. Values of response slops for interfering ions used to determine selectivity coefficients with the separate solutions method.

Ion	Response slope
Cl^-	-65.3 ± 0.7
NO_2^-	-60.1 ± 0.1
OAc^-	–61.5± 1.5

Table S2. Comparison of average nitrate concentrations during three copper and silver nanoparticle syntheses determined by the electrochemical nitrate sensor and colorimetric analysis.

Copper Nanoparticle Synthesis							
	Colorimetric			Ion Chromatography			Potentiometric
Time / (min)	$[NO_3^-]$ / (mM)	$[NO_2^-]$ / (mM)	Total $[NO_3^-]$ and $[NO_2^-]$/ (mM)	$[NO_3^-]$ / (mM)	$[NO_2^-]$ / (mM)	Total $[NO_3^-]$ and $[NO_2^-]$/ (mM)	Total $[NO_3^-]$ and $[NO_2^-]$/ (mM)
8	1.4 ± 0.4	0.03 ± 0.01	1.4 ± 0.4	1.82 ± 0.5	<0.04	1.8 ± 0.5	1.1 ± 0.3
20	3.1 ± 0.4	2.81 ± 0.6	6.0 ± 1.0	3.0 ± 0.6	3.0 ± 0.8	6 ± 1.4	2.5 ± 0.4
30	0.4 ± 0.2	0.3 ± 0.2	0.7 ± 0.4	0.6 ± 0.4	0.1 ± 0.1	0.7 ± 0.5	0.7 ± 0.3
40	0.26 ± 0.06	0.06 ± 0.03	0.32 ± 0.09	0.28 ± 0.01	<0.04	0.3 ± 0.1	0.08 ± 0.05
50	0.13 ± 0.04	0.01 ± 0.01	0.14 ± 0.05	0.22 ± 0.06	<0.04	0.22 ± 0.06	0.08 ± 0.03
60	0.12 ± 0.02	0.01 ± 0.01	0.14 ± 0.03	0.13 ± 0.02	<0.04	0.13 ± 0.02	0.06 ± 0.02

Silver Nanoparticle Synthesis							
	Colorimetric			Ion Chromatography			Potentiometric
Time / (min)	$[NO_3^-]$ / (mM)	$[NO_2^-]$ / (mM)	Total $[NO_3^-]$ and $[NO_2^-]$/ (mM)	$[NO_3^-]$ / (mM)	$[NO_2^-]$ / (mM)	Total $[NO_3^-]$ and $[NO_2^-]$/ (mM)	Total $[NO_3^-]$ and $[NO_2^-]$/ (mM)
8	3.1 ± 0.7	0.20 ± 0.03	3.29 ± 0.7	3.2 ± 0.9	0.11 ± 0.04	3.0 ± 1.0	3.2 ± 0.1
20	2.0 ± 2.0	1.6 ± 0.9	4.0 ± 3.0	3.0 ± 2.0	1.0 ± 1.0	4.0 ± 3.0	5.9 ± 0.2
30	0.07 ± 0.04	0.03 ± 0.01	0.10 ± 0.05	0.2 ± 0.5	0.20 ± 0.5	0.44 ± 0.10	0.03 ± 0.01
40	0.07 ± 0.04	0.03 ± 0.01	0.10 ± 0.05	0.2 ± 0.1	<0.04	0.17 ± 0.10	0.03 ± 0.01
50	0.06 ± 0.03	0.02 ± 0.01	0.08 ± 0.04	0.20 ± 0.08	<0.04	0.20 ± 0.08	0.06 ± 0.02
60	0.02 ± 0.01	0.02 ± 0.01	0.04 ± 0.02	0.2 ± 0.4	<0.04	0.17 ± 0.04	0.8 ± 0.3